Title:
Temporal Variations in the Photosynthetic Biosphere

Journal:
Science

PI:
Michael Behrenfeld

Popular Summary:
In this report, we describe results from the first 3 years of global SeaWiFS ocean chlorophyll and land plant measurements. This time period covered the end of one of the largest El Nino events in the past century and a strong La Nina. During this transition, terrestrial plant photosynthesis exhibited only a small change, whereas a significant increase in oceanic photosynthesis was observed. Latitudinal distributions of ocean production indicated that this increase in photosynthesis during the La Nina was distributed in the equatorial belt as well as in high production areas. The analysis also illustrated the large 'missing bloom' in ocean phytoplankton in the southern ocean. While land photosynthesis remained fairly steady during the third year of SeaWiFS measurements, ocean phytoplankton production continued to increase, albeit at a lower rate than from 1997 to 1999. Our results represent the first quantification of interannual variability in global scale ocean productivity.

Significant Findings:
An increase in ocean production during the first 3 years of the SeaWiFS mission; a strong hemispheric difference in the latitudinal distribution of ocean photosynthesis.

Temporal Variations in the Photosynthetic Biosphere

Michael Behrenfeld [1], James Randerson [2], Charles McClain [1], Gene Feldman [1], Sietse Los [3], Compton Tucker [1], Paul Falkowski [4], Christopher Field [5], Robert Frouin[6], Wayne Esaias [1], Dorota Kolber [5], & Nathan Pollack[7]

---

[1]National Aeronautic and Space Administration, Goddard Space Flight Center, Greenbelt, MD 20771

[2]California Institute of Technology, Divisions of Engineering and Applied Science and Geological and Planetary Sciences, Mail Stop 100-23, Pasadena, CA 91125

[3]Science Systems and Applications Incorporated, National Aeronautic and Space Administration, Goddard Space Flight Center, Greenbelt, MD 20771

[4]Institute of Marine and Coastal Sciences, Rutgers, The State University of New Jersey, New Brunswick, NJ 08901

[5]Carnegie Institution of Washington, Department of Plant Biology, 260 Panama Street, Stanford, CA 94305

[6]Scripps Institution of Oceanography, 8605 La Jolla Drive, La Jolla, CA 92037

[7]Hughes SDX, Goddard DAAC, National Aeronautic and Space Administration, Goddard Space Flight Center, Greenbelt, MD 20771

17 October 2000

Abstract: The Sea-viewing Wide Field-of-view Sensor (SeaWiFS) is the first remote sensing instrument to provide multi-year, global monthly measurements of both oceanic phytoplankton chlorophyll biomass (C_{sat}) and the Normalized Difference Vegetation Index (NDVI) of light harvesting on land. Global mean C_{sat} increased 8.6% per year between September 1997 and December 1998, reflecting altered nutrient distributions during an El Niño to La Niña transition, and then continued to increase at 2.2% per year from January 1999 to July 2000. Similar increases in global mean NDVI were not observed. Biospheric net primary production (NPP) for the 1997 to 2000 period increased 4.5% from 107.5 to 112.3 Pg C. Regionally, both land and ocean NPP exhibited strong year-to-year variability related to changes in precipitation, temperature, and ocean circulation.

Seasonal to decadal changes in the physical environment are manifested in the light harvesting capacity of plant communities throughout the biosphere and can be monitored remotely by changes in surface chlorophyll concentration (C_{sat}) in the oceans and the Normalized Difference Vegetation Index (NDVI) on land. A continuous, 20 year global record of satellite NDVI has permitted detection of interannual, climate-driven changes in terrestrial photosynthesis (*1-5*). An analogous long-term global record of C_{sat} does not exist. Measurements of C_{sat} were first made with the Coastal Zone Color Scanner (CZCS: 1978-1986), but this proof-of-concept sensor only collected data on an irregular basis and yielded incomplete global coverage of C_{sat} even after integration over the entire 8 year mission. The launch of SeaWiFS in 1997 marked the beginning of the first multi-year satellite measurements of phytoplankton biomass in 11 years, and has since provided greater global coverage in C_{sat} each month than was achieved throughout the lifetime of CZCS. SeaWiFS is also the first instrument with the spectral coverage and dynamic range to allow measurements of both C_{sat} and NDVI. Here we report spatial and temporal changes in C_{sat}, NDVI, and derived rates of net primary production (NPP) for the first 3 years of the SeaWiFS mission. Our results encompass a transition from El Niño to La Niña conditions, represent the first description of interannual variability in global phytoplankton biomass, and provide a basis for quantifying future responses of the photosynthetic biosphere to climate variability.

Our analysis is based on global, 4 km-resolution, monthly SeaWiFS C_{sat} and NDVI data collected between September 1997 and July 2000. Stability of the sensor has been accurately characterized from monthly lunar-based calibrations and derived products verified by comparison with field measurements (*6*). Biospheric NPP was estimated following the approach

of Field et al. (*7*), which integrates the Vertically Generalized Production Model (VGPM) for the oceans (*8*) with the Carnegie-Ames-Stanford Approach (CASA) for land (*9*). Variations in NPP for the CASA-VGPM model arise from changes in three factors: 1) photosynthetically active radiation (PAR), 2) the fraction of radiation absorbed by plants (related to C_{sat} and NDVI), and 3) light use efficiencies (ϵ). Coincident changes in these factors collectively control NPP. Therefore, unlike previous calculations based on temporally disjunct C_{sat}, NDVI, and ancillary fields (*7*), all data used in our current estimates of biospheric NPP were collected during the SeaWiFS period (*10*). The CASA-VGPM model was operated at a monthly time step.

Throughout the 3 year SeaWiFS record, temporal variability in C_{sat} was dominated by a pronounced seasonal cycle (Fig. 1). Summer phytoplankton blooms in the northern hemisphere exceeded those in the southern hemisphere, causing minima in global mean C_{sat} between November and March and maxima between May and September (Fig. 1A). Monthly anomalies clearly identified a secondary, interannual change in C_{sat} superimposed on this prominent seasonal pattern (Fig. 1A - right axis). Between September 1997 and December 1998, global mean C_{sat} increased at a rate of 8.6% per year in response to altered nutrient distributions resulting from an El Niño to La Niña transition (*11*). Changes in C_{sat} during this period were not uniform nor restricted to the equatorial belt, but rather entailed a general decrease in the areal extent of oligotrophic regions between 0.04 and 0.15 mgChl m^{-3}, an increase in mesotrophic blooms between 0.15 to 0.30 mgChl m^{-3}, and a decrease in phytoplankton biomass in the central ocean gyres. During the subsequent post-La Niña period of January 1999 to July 2000, C_{sat} continued to increase at the reduced rate of 2.2% per year, primarily reflecting net increases in phytoplankton biomass in the Pacific and Indian oceans. Unfortunately, lack of comparable

historical C_{sat} data forestalls deciphering whether this unprecedented increase represents true decadal-scale change or normal interannual variability

Like the oceans, temporal changes in land NDVI were dominated by strong seasonal fluctuations, with minima of 0.44 ± 0.01 (dimensionless) between December and February and maxima of 0.55 ± 0.01 between June and September (Fig. 1B). Significant regional changes in NDVI occurred throughout the SeaWiFS period, but increases in one region were compensated by equivalent decreases in another, such that global mean NDVI anomalies indicated little change even during the El Niño to La Niña transition (Fig. 1B - right axis). Over longer periods, historical NDVI data indicate that interannual variations can reach 70% in semi-arid regions (*4*) and up to 10% at high northern latitudes due to changes in the growing season (*5*). For the SeaWiFS record, the striking difference in temporal anomalies of C_{sat} and NDVI (Fig. 1) suggests an enhanced global-scale sensitivity of phytoplankton biomass to interannual variability in environmental forcings.

Annual global NPP increased from 107.5 to 112.3 Pg C (Pg = 10^{15} g) between September 1997 and July 2000 based on the CASA-VGPM biosphere model, with net carbon fixation increasing by 0.9 Pg on land and 3.9 Pg in the oceans. Our estimated biospheric NPP is higher than the CASA-VGPM estimate of 104.9 Pg C y^{-1} reported by Field et al. (*7*) for remote sensing data collected between 1978 and 1990. This difference largely reflects an increase in ocean NPP that cannot be unequivocally attributed to either a true change in ocean biology or simply better remote sensing data. What is certain is the difference does not reflect divergent approaches to NPP modeling or a drift in sensor calibration, since C_{sat} values did not uniformly increase globally.

On land, NPP peaks between 15°S and 10°N, reaching 87.1 gC m^{-2} $month^{-1}$, and then exhibits a hemispherically-asymmetric dependence on latitude and season (Fig. 2A). In the northern hemisphere, continental climatic influences dominate precipitation and temperature patterns and give rise to extensive arid regions of low NPP between 15°N and 35°N. At southern latitudes, a similar NPP minimum occurs, but is restricted to the 20°S to 30°S band due to relatively greater maritime climatic influences (Fig. 2A). Strong seasonality in NPP at >35°N over the large continental areas of North America and Eurasia is the basis for the prominent seasonal cycle in NDVI (Fig. 1B). A secondary, moderately-seasonal peak in southern hemisphere NPP also exists between 30°S and 58°S, but has little influence on global mean NDVI patterns due to the small land area of this region.

For the oceans, seasonal variability in the latitudinal distribution of NPP in the southern hemisphere is nearly a perfect mirror image of the northern hemisphere, except from 40°S to 75°S between October to April. From 35°N to 35°S, ocean NPP exhibits little seasonality and ranges from a maximum of 20.9 gC m^{-2} $month^{-1}$ in the equatorial upwelling belt to a minimum of 8.2 gC m^{-2} $month^{-1}$ in the low-nutrient, central ocean gyre region (Fig. 2B). At >40°N, NPP is strongly seasonal, varying from 0 to 49.1 gC m^{-2} $month^{-1}$ (Fig. 2B). In this region, phytoplankton growth is generally light-limited during winter months, due to deep mixing and low incident PAR, and increases dramatically during the summer when surface waters rich in nutrients become stratified and PAR is high. In the southern hemisphere, a corresponding mid-summer maximum in NPP at >40°S is not observed. Instead, seasonality is greatly dampened and NPP actually *decreases* from 27.4 to 7.1 gC m^{-2} $month^{-1}$ between 40°S and 70°S (Fig. 2B). This absence of a high-latitude, mid-summer bloom in the southern ocean results from a lack of

seasonality in the environmental factor(s) limiting phytoplankton growth, most likely iron and light (*12-14*). For the 40°S to 75°S region, we calculated that an 8.9 Pg C y^{-1} increase in ocean NPP would result if seasonal changes in phytoplankton biomass paralleled those of the northern hemisphere.

Distributions of biospheric NPP register spatial and seasonal changes in light, soil moisture, nutrient availability, and temperature (Fig. 3A,B). Seasonal variability in northern hemisphere terrestrial NPP is particularly strong due to greater variability in these growth limiting factors compared to the southern hemisphere or the oceans (Fig. 3A,B). Although global-scale interannual changes in NDVI were small relative to C_{sat} for the September 1997 to July 2000 period (Fig. 1B), both land and ocean NPP displayed significant regional variability related to local precipitation, temperature, and ocean circulation changes. For the December to February season, the 1997-1998 El Niño to La Niña transition involved an increase in upwelling and NPP in the eastern equatorial Pacific (*11*), as well as a deepening of the nutricline and consequential decrease in NPP in the western Pacific (Fig. 3C). Southern gyres of the Atlantic and Pacific oceans also exhibited a decrease in NPP during the transition, while a large increase occurred in the south Atlantic subtropical convergence east of Argentina. On land, increased precipitation over eastern Africa broadly increased NPP during the El Niño period and reflected changes in Indian ocean circulation that simultaneously decreased phytoplankton productivity in the northeast while increasing NPP west of Indonesia (*15*) (Fig. 3C). Likewise, changes in precipitation over South America enhanced NPP from southern Brazil through Argentina during El Niño conditions, while decreasing productivity in upper Amazonia. Coherence between circulation patterns and interannual NPP anomalies was also evident for the 1998-1999 June to

August season (Fig. 3D); particularly, the temperature-related decrease in NPP over the Soviet Union and increase over Europe, the moderate increase in ocean NPP in the northern hemisphere gyres, and the peculiar decrease in equatorial Pacific NPP bordered by symmetric increases both to the north and south.

Elemental cycling through the photosynthetic biosphere has and will have a profound influence on climate variability. Global observations of light harvesting capacities in land and ocean plants fosters an understanding of the links between biogeochemical and ecological processes, so evident in maps of NPP and its interannual anomalies (Fig. 3). Continuation of such measurements over prolonged periods also allows decadal and longer-term changes to be resolved from normal, larger-amplitude seasonal and interannual cycles. The SeaWiFS record now permits a comprehensive assessment of biospheric NPP and documents for the first time multi-year temporal changes in global phytoplankton biomass (Fig. 1). Of our estimated >100 Pg C y^{-1} photosynthetically fixed between 1997 and 2000, less than 3% was sequestered in long-term carbon pools (*16*). Over an annual period, the remaining organic carbon is released back to the atmosphere as respiratory CO_2. Differences in the temporal coupling of primary production and respiration influence the atmospheric signature of land and ocean photosynthesis. Although latitudinal NPP distributions for both systems (Fig. 2) are consistent with hemispheric differences in the seasonal amplitude of atmospheric CO_2 cycles, the rapid turnover of phytoplankton biomass, along with the buffering effect of oceanic carbonate chemistry, causes land NPP to dominate seasonal cycles in atmospheric CO_2 (*17, 18*). In contrast, both components contribute to longer-term carbon sequestration, but quantifying this land-ocean partitioning will require further improvements in ϵ models and better characterization carbon of

remineralization pathways. As these improvements are realized, continuation of global SeaWiFS measurements will provide a basis for assessing changes in Earth system carbon cycling.

REFERENCES

1. R. B. Myneni, S. O. Los, C. J. Tucker, *Geophys. Res. Letters* **23,** 729 (1995)

2. P. Maisongrande, A. Ruimy, G. Dedieu, B. Saugier, *Tellus*, **47B**, 178 (1995)

3. R. B. Myneni, C. D. Keeling, C. J. Tucker, G. Asrar, R. R. Nemani, *Nature*, **386,** 698 (1997)

4. C. J. Tucker, S. N. Nicholson, *Ambio,* **28**, 587 1999)

5. R. B. Myneni, C. J. Tucker, C. D. Keeling, G. Asrar. *J. Geophys. Res.* **103,** 6145 (1998)

6. The SeaWiFS sensor is mounted on the OrbView-2 spacecraft (*19*) and follows a sun-synchronous orbit with a noon-time equatorial crossing. The sensor provides complete 4-km global coverage every 2 days. The mission has operationally produced oceanic, atmospheric, and terrestrial data products since September 1997. The complete SeaWiFS data set has been reprocessed three times to incorporate refinements in sensor calibration, atmospheric correction, and bio-optical algorithms. The present study uses data from the most recent, May 2000 reprocessing (*20*). Monthly lunar calibration images indicate a progressive decrease in sensitivity of <1% for the 6 visible wavebands and up to 10% for the near infrared wave bands. By applying calibration corrections based on the lunar time series, temporal changes in radiometric sensitivity are corrected to within <1% (*20, 21*). Comparison of SeaWiFS derived C_{sat} values and 103 coincident in situ measurements indicated an average difference of <6% (RMS error = 0.301) for surface chlorophyll concentrations between 0.029 and 6.42 mg m^{-3} (*20*). Corrections to NDVI values were applied for time-series outliers, missing data during winter, and cloud effects in tropical forests (*22, 23*).

7. C. B. Field, M. J. Behrenfeld, J. T. Randerson, P. G. Falkowski, *Science* **28**, 237 (1998).

8. M. J. Behrenfeld, P. G. Falkowski. *Limnol. Oceanogr.* **42**,1 (1997).

9. C. S. Potter *et al.*, *Global Biogeochem. Cycles* **7**, 811 (1993)

10. For the oceans, ϵ was modeled as a function of sea surface temperature (*8*). For land, the fraction of PAR absorbed by vegetation was calculated from NDVI (*23*) and ϵ was related to local variations in soil moisture and temperature. For the oceans, sea surface temperature fields were provided by coincident Advanced Very High-Resolution Radiometer (AVHRR) measurements. Monthly, 9-km resolution PAR fields were obtained from 5 SeaWiFS visible wavebands using an algorithm adapted from Frouin & Chertock (*24*). For land, PAR was taken as the sum of direct and diffuse radiation from monthly maps provided by NCEP (*25*). Local soil moisture and temperature fields were obtained from NCEP monthly precipitation and 2m air temperature maps.

11. F. P. Chavez *et al.*, *Science* **286**, 2126 (1999)

12. B. G. Mitchell, E. A. Brody, O. Holm-Hansen, J. Bishop. *Limnol. Oceanogr.* **36**, 1662 (1991)

13. C. W. Sullivan, K. R. Arrigo, C. R. McClain, J. C. Comiso, J. Firestone, *Science* **262**, 1832 (1993)

14 P. Boyd et al., *Nature* (in press)

15. R. G. Murtugudde, S. R. Signorini, J. R. Christian, A. J. Busalacchi, C. R. McClain, *J. Geophys. Res.* **104**, 18,351 (1999).

16. J. L.Sarmiento, S. C. Wofsy A U.S. Global Carbon Cycle Plan. (U.S. Global Change Research Program, Washington D.C. 1999)

17. C. D. Keeling, J. F. S. Chin, T. P. Whorf, *Nature*, **382**, 146 (1996)

18. T. J. Conway, T.J. *et al. J. Geophys. Res.* **99**, 22,831 (1994).

19. S. B. Hooker, W. E. Esaias, *Eos* **74**, 241 (1993).

20. *NASA Technical Memorandum 2000-206892, Vol. 9-11*, NASA, Maryland (2000).

21. R. A. Barnes, R. E. Eplee, F. S. Patt, C. R. McClain, *Appl. Opt.* **38** 4649 (1999).

22. P. J. Sellers *et al.*, *J. Climate* **9** 706 (1996).

23. S. O. Los *et al.*, *J Hydromet.* **1** 183 (2000).

24. R. Frouin, B. Chertock, *J. Appl. Meteor.*, **31** 1056 (1992).

25. NCEP Reanalysis data were provided by the NOAA-CIRES Climate Diagnostics Center, Boulder, Colorado, USA, from their Web site at http://www.cdc.noaa.gov/

26. *Acknowledgments*: The authors thank members of the SeaWiFS Project Office and Orbimage Orbview-1 support staff for their diligent effortsin assuring the success of the SeaWiFS mission and NASA Headquarters for supporting the SeaWiFS project.

Figure Legends

1. Global monthly means and anomalies in surface ocean chlorophyll (C_{sat}: mgChl m^{-3}) and land NDVI (dimensionless) for SeaWiFS measurements between September 1997 and July 2000. Anomalies were calculated as the difference between C_{sat} or NDVI for a given month and the average value for that month during the 3 year time series. (A) ● = Monthly mean C_{sat} in mgChl m^{-3} (left axis). ◊ = monthly anomaly (right axis). (B) ● = Monthly mean NDVI (dimensionless; left axis). ◊ = monthly anomaly (right axis).

2. Seasonal average NPP (gC m^{-2} $month^{-1}$) for the 3 year SeaWiFS time series as a function of latitude. (A) Terrestrial NPP for (dashed line) December through February and (solid line) June through August. The labeled, dotted line at >16°S shows the corresponding NPP values from the northern hemisphere to illustrate differences in Austral and Boreal summers. (B) Ocean NPP for (dashed line) December through February and (solid line) June through August. As in (A), the labeled dotted line at > 40°S shows corresponding NPP values from the northern hemisphere. The difference between the dotted and solid lines between 40oS and 75oS illustrates the large 'missing' bloom in the southern hemisphere during the Austral summer.

3. Average biospheric NPP and interannual differences for Austral (December to February) and Boreal (June to August) summers. NPP (gC m^{-2} $month^{-1}$) was estimated using SeaWiFS data and the integrated CASA-VGPM biospheric model (*7*). (A) Average NPP for the 1997 El Niño and 1998 La Niña Austral summers. (B) Average NPP for the 1998

La Niña and 1999 post-La Niña Boreal summers. (C) Austral summer NPP for 1997 minus 1998. (D) Boreal summer NPP for 1998 minus 1999. Red and blue colors in (C) and (D) denote increases and decreases in NPP, respectively.

Figure 1

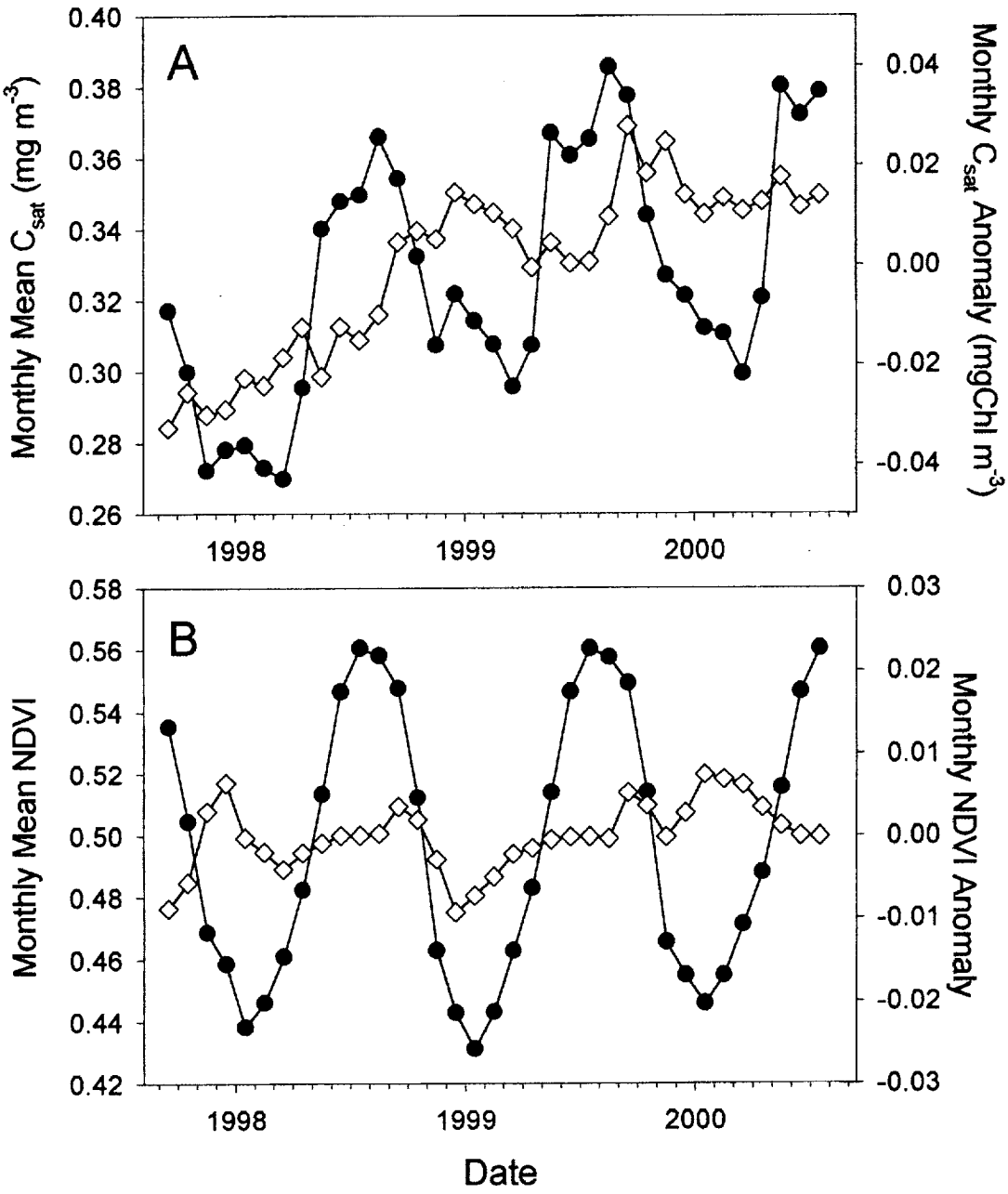
A
B
Monthly Mean C_{sat} (mg m^{-3})
Monthly C_{sat} Anomaly (mgChl m^{-3})
Monthly Mean NDVI
Monthly NDVI Anomaly
0.40
0.38
0.36
0.34
0.32
0.30
0.28
0.26
0.04
0.02
0.00
-0.02
-0.04
0.58
0.56
0.54
0.52
0.50
0.48
0.46
0.44
0.42
0.03
0.02
0.01
0.00
-0.01
-0.02
-0.03
1998
1999
2000
Date

Figure 2

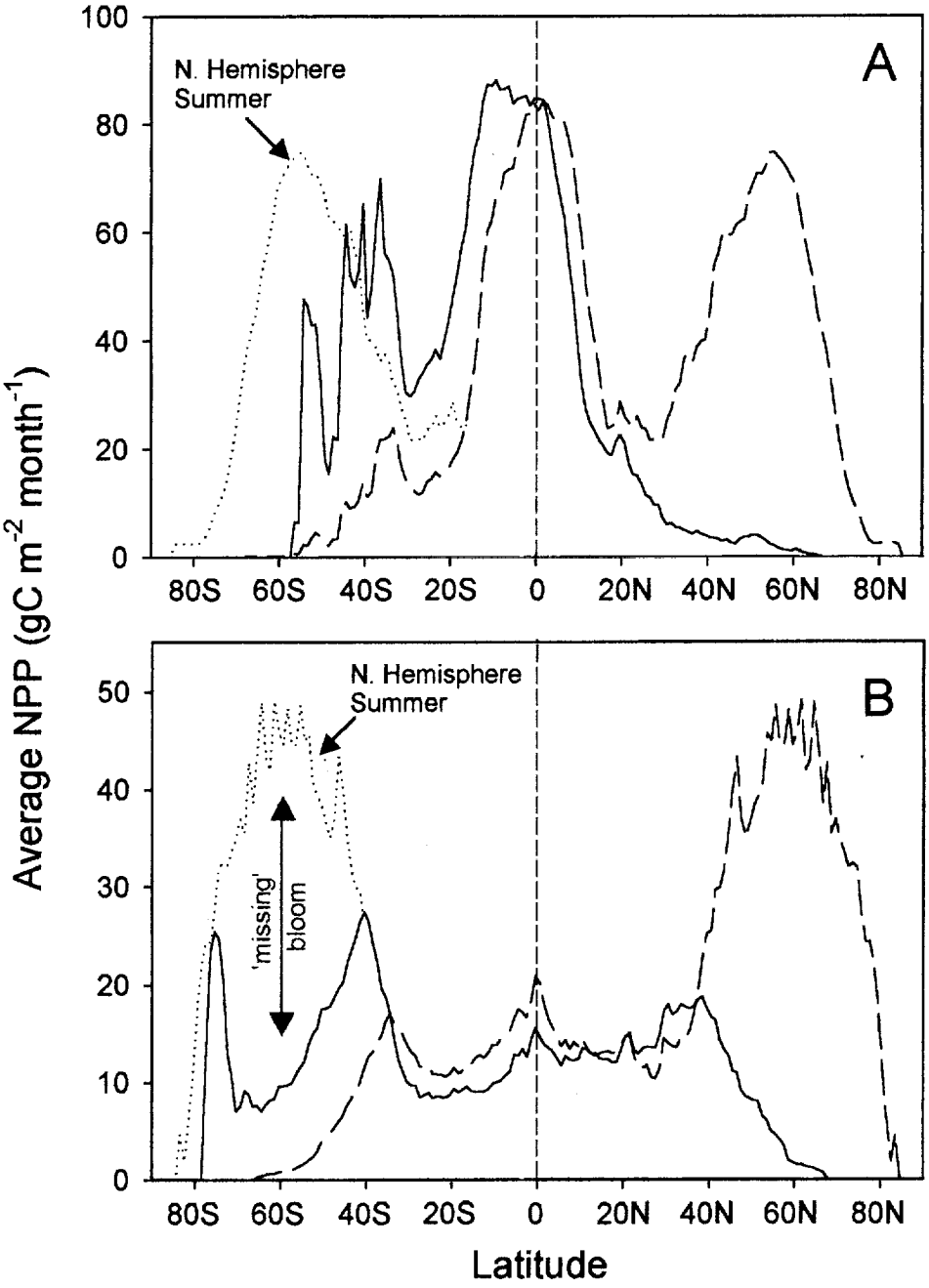
A
N. Hemisphere Summer
100
80
60
40
20
0
80S 60S 40S 20S 0 20N 40N 60N 80N
B
N. Hemisphere Summer
'missing' bloom
50
40
30
20
10
0
80S 60S 40S 20S 0 20N 40N 60N 80N
Latitude
Average NPP (gC m-2 month-1)

Figure 3

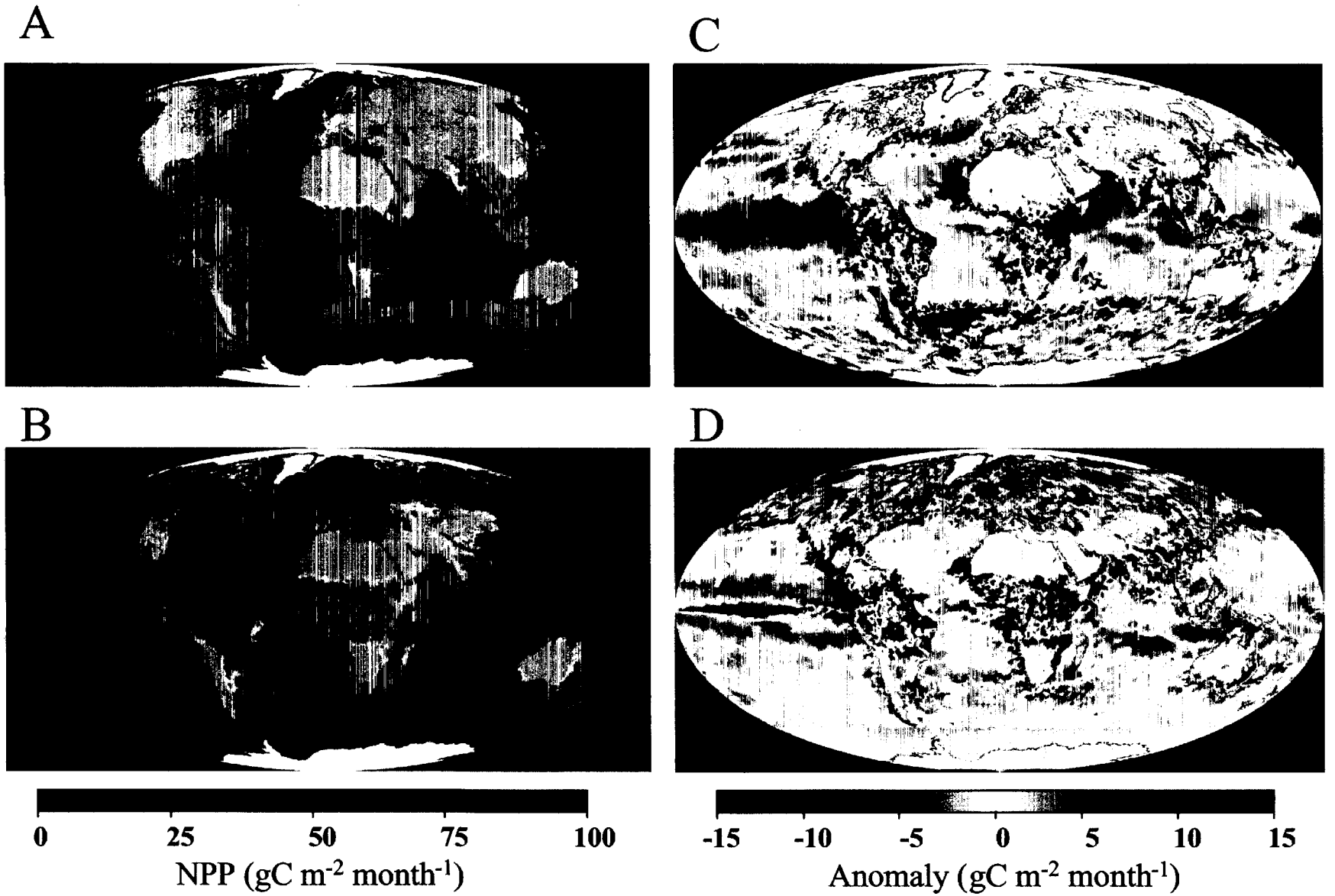
A
C
B
D
0
25
50
75
100
NPP (gC m-2 month-1)
-15
-10
-5
0
5
10
15
Anomaly (gC m-2 month-1)